Supplementary material for CDS

Table 2 shows the B_c^+ meson signal yield in each $(p_{\rm T}, y)$ bin.

Table 2: B_c^+ meson yield in each $p_{\rm T}$ and y bin, with the statistical uncertainty from the fit to the invariant mass distribution.

$p_{\rm T}$(GeV/c)	$2.0 < y < 2.9$	$2.9 < y < 3.3$	$3.3 < y < 4.5$
$0 < p_{\rm T} < 2$	88.7 ± 12.6	100.2 ± 13.1	78.3 ± 14.1
$2 < p_{\rm T} < 3$	100.1 ± 12.3	103.7 ± 12.9	106.6 ± 13.5
$3 < p_{\rm T} < 4$	103.1 ± 12.7	93.6 ± 13.1	124.4 ± 14.2
$4 < p_{\rm T} < 5$	142.6 ± 14.2	93.1 ± 11.3	166.9 ± 15.9
$5 < p_{\rm T} < 6$	145.9 ± 13.9	107.4 ± 12.7	136.6 ± 15.3
$6 < p_{\rm T} < 7$	113.2 ± 12.4	107.1 ± 11.7	91.9 ± 11.0
$7 < p_{\rm T} < 8$	111.2 ± 11.7	66.8 ± 9.8	76.6 ± 10.4
$8 < p_{\rm T} < 10$	149.3 ± 13.9	71.5 ± 9.7	122.3 ± 12.9
$10 < p_{\rm T} < 14$	144.0 ± 13.2	89.4 ± 10.8	80.3 ± 10.5
$14 < p_{\rm T} < 20$	81.2 ± 9.6	34.5 ± 7.7	29.2 ± 6.7

The results are compared with the theoretical predictions in Fig. 5 and Fig. 6. For B_c^+ meson the predictions following the α_s^4 approach [40] are shown. We use the CTEQ6LL [49] parton distribution functions, and the leading order running α_s, the characteristic energy scale $Q^2 = {p_{\rm T}}^2 + m^2_{B_c^+}$, and the masses of the b and c quarks are set to $m_b = 4.95\,{\rm GeV}/c^2$ and $m_c = 1.326\,{\rm GeV}/c^2$. The normalization of the theoretical predictions uses $0.47\,\mu{\rm b}$ as the B_c^+ production cross-section in the whole phase space and 0.33% for $\mathcal{B}(B_c^+ \to J/\psi\,\pi^+)$ [50], corrected for the latest measurement of the B_c^+ lifetime. The theoretical prediction on the B^+ cross-section is based on the fixed order + next-to-leading log (FONLL) framework [51]. The uncertainties on the theory curves are the uncertainties of the FONLL calculation, including the uncertainties of the b quark mass, the renormalisation and factorisation scales, and CTEQ6.6 [52] functions. The FONLL predictions are scaled according to the measured branching fraction value $\mathcal{B}(B^+ \to J/\psi\,K^+) = 0.106\%$ [34] and the B^+ production cross-section $38.9\,\mu{\rm b}$ measured at $\sqrt{s} = 7\,{\rm TeV}$ [53] increased by 20% due to higher collision energy [54].

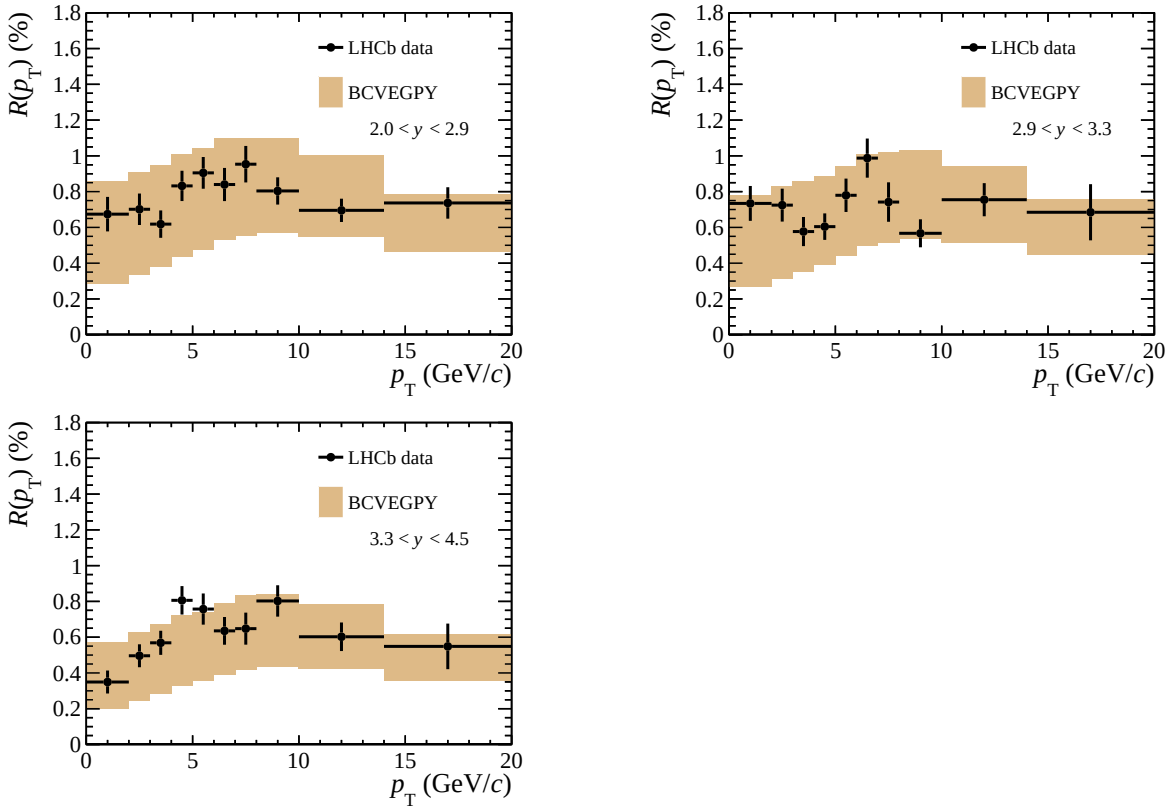

Figure 5: Ratio $R(p_{\rm T}, y)$ as a function of $p_{\rm T}$ in the regions $2.0 < y < 2.9$ (*top left*), $2.9 < y < 3.3$ (*top right*), and $3.3 < y < 4.5$ (*bottom left*), with theoretical predictions following the α_s^4 approach [40] overlaid.

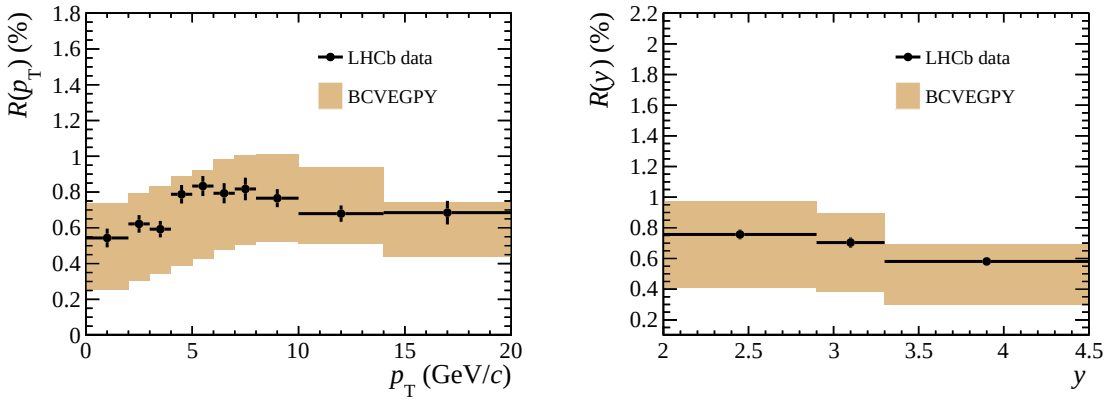

Figure 6: Ratio $R(p_{\rm T})$ as a function of $p_{\rm T}$ integrated over y in the region $2.0 < y < 4.5$ (*left*) and $R(y)$ as a function of y integrated over $p_{\rm T}$ in the region $0 < p_{\rm T} < 20\,{\rm GeV}/c$ (*right*) are compared to the theoretical predictions following the α_s^4 approach [40].